

# MONITORING THE CARBON STORAGE OF URBAN GREEN SPACE BY COUPLING RS AND GIS UNDER THE BACKGROUND OF CARBON PEAK AND CARBON NEUTRALIZATION OF CHINA

*Xueying Mo & Rueti-Yuan Wang*

*Research Scholar, Guangdong University of Petrochemical Technology, Sch Sci, Maoming 525000, Peoples R China*

**Received: 15 Aug 2022**

**Accepted: 17 Aug 2022**

**Published: 23 Aug 2022**

## **ABSTRACT**

*Based on the background of Carbon Peak and Carbon Neutralization (CPCN), this study aims to apply Remote Sensing (RS) images of Shenzhen in 2008, 2013 and 2018, combined with RS and Geography Information System (GIS) technology to classify Land Use/Land Cover (LULC), calculate Net Primary Productivity (NPP), and then estimate the carbon storage of green space in Shenzhen. The results show that during the decade from 2008 to 2018, the green space in Shenzhen is reduced and the construction land has increased. In the process of land transfer in Shenzhen, both cultivated land is non-agricultural and the reclamation of construction land is withdrawn, green space carbon reserves decreased in the beginning and then increased. The reason is that green space was transformed into other types of land from 2008 to 2013, resulting in the reduction of green space carbon storage. However, the change of green space from 2013 to 2018 is not obvious. Due to Shenzhen advocates a low-carbon economy and green development, resulting in an increase in carbon storage.*

**KEYWORDS:** *Net Primary Productivity (NPP); Land Use/Land Cover (LULC); Remote Sensing (RS); Carbon Storage; Climate Change*

## **INTRODUCTION**

In the process of industrialization, greenhouse gas emissions dominated by carbon dioxide cause global warming and various accompanying extreme weather and natural disasters (Bonneuil et al., 2021; Cheng, et al., 2022; Fan and Wei, 2022; Quevauviller, 2022; Tao et al., 2022). Reducing greenhouse gas emissions has become the common responsibility and obligation of all countries. Facing a series of environmental problems caused by global climate change, the Paris Agreement clearly proposes to keep the global average temperature rise within 2 °C relative to the pre-industrialization level by the end of this century, and make efforts to control the global average temperature rise within 1.5°C to reduce the risk and impact of climate change (Choudhury et al., 2022; Sun et al., 2022; Peng et al., 2022; Yu et al., 2022).

Following the trend of the times, China proposed in 2020 to strive for a national strategy to achieve the goal of carbon peak by 2030 and carbon neutralization by 2060(CPCN); (Qian, et al., 2022). Commonly, there are two ways to achieve carbon neutralization: one is to reduce carbon emissions, the other is to pay attention to the carbon sequestration of natural ecosystems (Li, 2021). Studies show that strengthening the carbon sequestration capacity of natural ecosystems is one of the most economical and effective ways to offset and absorb carbon emissions (Yang et al., 2022).

With the development of China on urbanization policy, the control and monitoring of urban carbon emissions have a high correlation between CPCN (Shen et al., 2021; Imani et al., 2022; Tao et al., 2022). Due to the high degree of human activities and agglomeration in cities, besides causing a series of urban heat island effect, urban air quality, urban ecosystem change, also they have a high carbon emission effect (Mahamba, et al., 2022). Therefore, how to pay attention to and solving the problem of urban carbon emission is an important indicator of government policy. Generally, green space, lakes, wetlands and other natural ecosystems have strong carbon sequestration capacity (Byomkesh et al., 2012; Dan-jumbo et al., 2018; Chen et al., 2019; Aka et al., 2022; Zhang et al., 2022). Besides contributing to the protection of urban ecology, its function also plays an important role in the cultural adjustment of living activities and leisure, and is also an important indicator of sustainable urban development. Thus, making good use of these carbon sequestration ecological spaces in the city will contribute to the monitoring and control of urban carbon emissions, and promote the policy of CPCN (here in after referred to as the “dual carbon” goal) (Qian, et al., 2022).

Urban green space, in a broad sense, refers to all areas covered by vegetation within the city. As an important part of the urban ecosystem, urban green space can fix carbon and produce oxygen, and effectively alleviate the heat island effect. It is the main direct carbon sink way of the city. Carbon sink refers to the process, activity and mechanism of removing carbon dioxide from the air. Carbon sink in the terrestrial ecosystem mainly refers to the amount of carbon dioxide absorbed and stored by forests (Li, 2021), or the capacity of forests to absorb and store carbon dioxide. By enhancing the carbon sink function of urban green space, the city can achieve carbon and oxygen balance, or alleviate the carbon sink pressure of forest land outside the city, it helps to reduce the significant impact on production, life and ecology due to the increase of carbon dioxide concentration, and plays an important role in achieving the goal of "CPCN" (Shen et al., 2021; Yu and Wang, 2021; Qian, et al., 2022; Zhang and Zhou, 2021) Therefore, the quantitative study of carbon storage in urban green space has guiding theoretical and practical significance (Wang et al., 2022).

As the first batch of low-carbon pilot cities, carbon emission trading pilot cities and sustainable development agenda Innovation Demonstration Zone (IDZ), Shenzhen has guiding significance for China's economic construction and development, low-carbon environment and green city. It is also the worthwhile study area of this paper. Thus, this study takes Shenzhen as the research area, uses Remote Sensing (RS) data and technology to realize LULC classification through Support Vector Machine (SVM) supervised classification method (Mirik et al., 2013; Chen, 2019; Talukdar et al., 2020; Xiong et al., 2020; Liou et al., 2021), meanwhile uses meteorological data as the data source to estimate Net Primary Productivity (NPP) through Carnegie-Ames-Stanford Approach (CASA) model (Potter et al., 1993 ; Field et al., 1995; Li et al., 2012), and finally using the vegetation-carbon-sequestration model to estimate the carbon storage of Shenzhen.

This study is organized as follows: literature reviews are first presented, that refers to the main theory, concepts and technological trends in this study. In the following section, the study area and analysis methods as well as process framework are presents, along with data processing. The fourth and fifth section layout the analysis results of LULC change and the carbon store on the study area, then to figure out what's real condition happen. Finally, a summary of the discovery on the monitoring benefits of this study and describing the contribution significance.

## LITERATURE REVIEW

### Carbon Storage of Urban Green Space

As the most concentrated area of human life, cities account for a large part of carbon dioxide emissions. Meanwhile, with the acceleration of urbanization, carbon dioxide emissions are increasing. Studies show that 97% of carbon dioxide emissions come from urban areas. Thus, it is urgent to study the carbon sources and sinks of cities to provide decision-making basis for urban green and low-carbon development. Urban green space is one of the factors to increase urban carbon sequestration, so the quantitative research on the carbon sequestration capacity of urban green space is of great significance (Shen et al., 2021; Zhang et al., 2022). Generally, relevant research on carbon storage estimation of the forest ecosystem was carried out with the help of ecological methods (Guan et al., 1998; Kashaigili et al., 2013; Wang et al., 2022). Carbon storage is the reserve amount of carbon element, the quality of carbon element or the amount of material, usually refers to the amount of carbon in a carbon pool (forest, ocean, land, etc.) (Wang et al., 2021; Wang et al., 2022). At first, the methods mainly include sample land inventory methods and biomass model methods. In terms of biomass also known as plant biomass, it refers to the dry weight of organic matter contained in unit area at a certain time. Later, it was gradually transformed into the measurement of carbon storage and carbon sink combined with RS technology (Yang et al., 2005; Lu et al., 2008; Wang et al., 2021; Zhang et al., 2022). RS satellites and other technologies can dynamically acquire their change information in real time by means of space-time monitoring, which will play an efficient regulatory role in maintaining ecology and promoting carbon absorption.

In the estimation of green space carbon reserves, the study is based on the estimation of forest carbon reserves first. After the measurement of forest biomass, the forest carbon reserves are converted at a certain proportion. The research on forest carbon reserves was first carried out in Germany, and then Japan, the United Kingdom and the United States gradually joined the ranks of carbon reserves estimation. Nowak (1993) estimated the total carbon reserves of American cities; Jo and McPherson (1995) estimated the carbon absorption and release of green space in Chicago residential area; Rowntree and Nowak (1991) estimated the carbon storage of urban forests in the whole United States; Myeong et al. (2006) used RS technology to estimate the aboveground carbon reserves of urban forests in New York City by establishing a relationship model between NDVI and aboveground forest carbon reserves of urban forests. Bordoloi et al. (2022) used an integrated satellite-based approach to model space carbon stocks and carbon sink potential for different LULC patterns in northeast India.

The research on carbon storage in China started to get involved in development in recent years. That is, with the continuous attention to global climate change, Chinese scholars have also started to study and estimate the carbon storage and carbon dioxide absorption benefits of urban forests. Such as Guan et al. (1998) outweigh the green space carbon storage in the built-up area of Guangzhou by using the measured data; Han et al. (2003) introduced the application of RS and GIS technology in modern urban green space, and applied remote sensing and GIS technology to evaluate the ecological benefits of urban vegetation. Zhou et al. (2010) proposed an estimation model of carbon sequestration of urban green space vegetation based on remote sensing data in, and used the model to estimate the aboveground dry biomass and aboveground net primary productivity of urban green space vegetation.

## The NPP and CASA

The Net Primary Productivity (NPP) of vegetation refers to the carbon absorbed by green plants through photosynthesis to remove carbon from their own respiration (Deng et al., 2022; Zhang et al., 2022). The remaining organic part can reflect the carbon fixation capacity of plants. It is of great significance for tracking regional carbon reserves, studying the carbon cycle, and helping to achieve “CPCN” (Xu et al., 2019; Zhang and Zhou, 2021). In terms of Carbon Peak, that is, the peak of carbon emission refers to the peak amount of carbon dioxide (or other major greenhouse gases) artificially discharged into the atmospheric environment at a certain time point (period). Additionally, Carbon Neutralization is also known as net zero carbon emission or net zero carbon footprint, its concept is divided into narrow and broad sense. Carbon neutralization refers to the net zero emission of carbon dioxide, but it is not the complete absence of carbon dioxide emissions, but the long-term balance between emissions and absorption. In a broad sense, carbon neutralization means not only carbon dioxide but also other major greenhouse gases (such as CH<sub>4</sub>, N<sub>2</sub>O, SF<sub>6</sub>, etc.) should reach net zero emissions.

As for the studies of NPP, the method of sample investigation and inventory was first used, focusing on the role of ecosystems in the carbon cycle with the method of biomass. With the development of time and technology, RS technology was introduced into relevant research, and RS technology can quickly and efficiently obtain the basic data of regional and large-scale ecosystems.

In recent years, with the development of spatial analysis technologies such as RS and GIS (Amraoui et al., 2022; Uwiringiyimana and Choi, 2022; Zhao and Du, 2022), the light energy utilization model driven by RS data has developed rapidly, with CASA model as a typical representative. The combination of light energy utilization model represented by CASA model and RS technology provides convenience for the study of NPP model. The CASA model is widely used to estimate NPP at present. The CASA model builds an RS parameter model based on the mechanism of vegetation photosynthesis. After inputting meteorological data, land area, photosynthetic effective radiation of vegetation, coverage status and other parameters, it can estimate regional land NPP and global carbon cycle. It estimates NPP through RS data and meteorological data, which not only avoids the collection of complex parameters, but also can accurately simulate a wide range of NPP. In addition, the RS data adopted has strong periodicity, wide observation area and high spatial-temporal resolution, making it become a main method for estimating NPP and carbon reserves of forest ecosystem (Potter et al., 1993; Wang, 2021; Zhang et al., 2022)

The research on the NPP of vegetation in China mainly began after 1970. Such as Piao et al. (2003) estimated the NPP of vegetation in the Yangtze River Basin; Zhu et al. (2005) estimated the NPP of vegetation in Inner Mongolia, China; it is concluded that the carbon sequestration benefits produced by forests play an important role in the global carbon cycle; Liet et al. (2015) estimated the carbon reserves of Shangri-La based on CASA model; Abdureyimu (2018) used the CASA model to inverse the NPP value of Ili Valley, calculated the vegetation carbon storage using empirical model, and analyzed the temporal and spatial distribution characteristics of vegetation carbon storage in Ili Valley.

## STUDY AREA AND METHODS

### Site Description

Shenzhen, a prefecture level city under the jurisdiction of Guangdong Province, is a sub provincial city, specifically designated in the national plan, a megacity, and a special economic zone, a national economic center, an international city,

a scientific and technological innovation center, a regional financial center, and a trade and logistics center approved by the State Council. Shenzhen has nine administrative districts and one new district: such as Luohu District, Futian District, Nanshan District, Baoan District, Longgang District, Yantian District, Longhua District, Pingshan District, Guangming district and Dapeng new district (show as Figure1).

Shenzhen, a coastal city in southern China, is located in the south of the Tropic of cancer. It is located at  $113^{\circ} 46'$  to  $114^{\circ} 37'E$  and  $22^{\circ} 27'$  to  $22^{\circ} 52' N$  in the south of Guangdong Province, on the east bank of the Pearl River Estuary, adjacent to Daya Bay and Dapeng Bay in the East; It is adjacent to the Pearl River Estuary and Lingdingyang in the West. Shenzhen River is connected with Hong Kong in the South. It borders Dongguan and Huizhou in the north. Since the 40 years of reform and opening up, Shenzhen has grown transform a small fishing village to an international metropolis step by step, from a traditional agricultural area become a global urbanization area, creating an urbanization miracle of "Shenzhen speed"(Wu et al., 2020).Becoming one of the four major central cities in Guangdong, Hong Kong, Macao, Dawan District, a national logistics hub, an international comprehensive transportation hub, an international science and technology industry innovation center, and one of China's three national financial centers, it will spare no effort be building a leading demonstration area of socialism with Chinese characteristics, a comprehensive national science center and a global marine center.

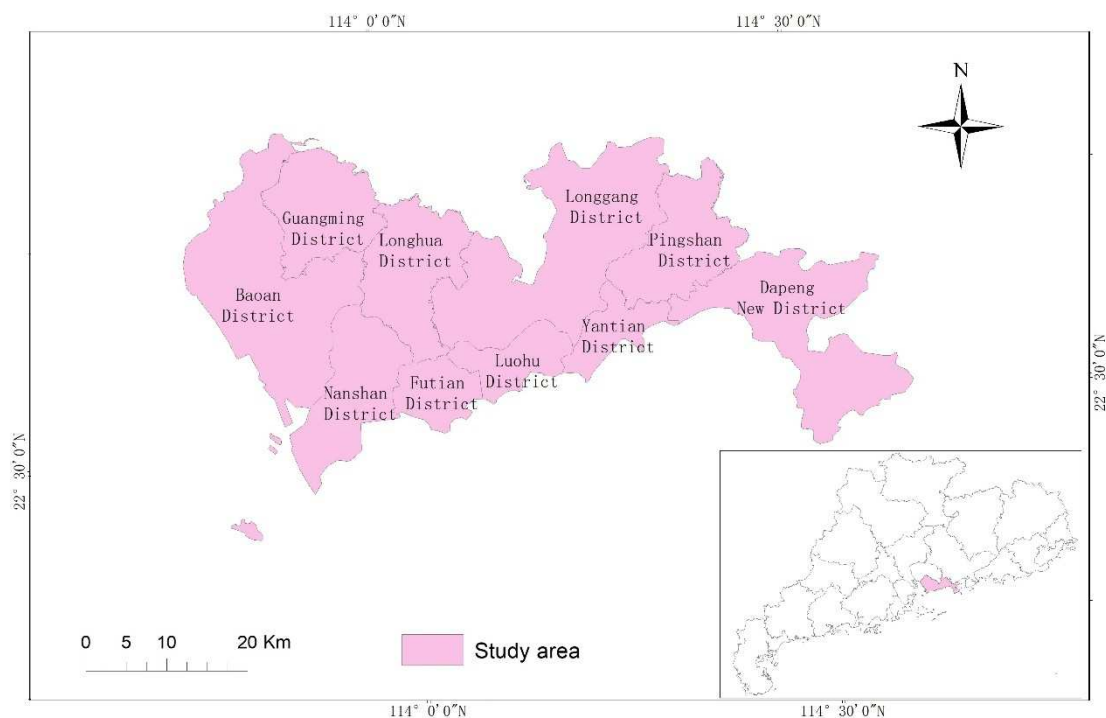
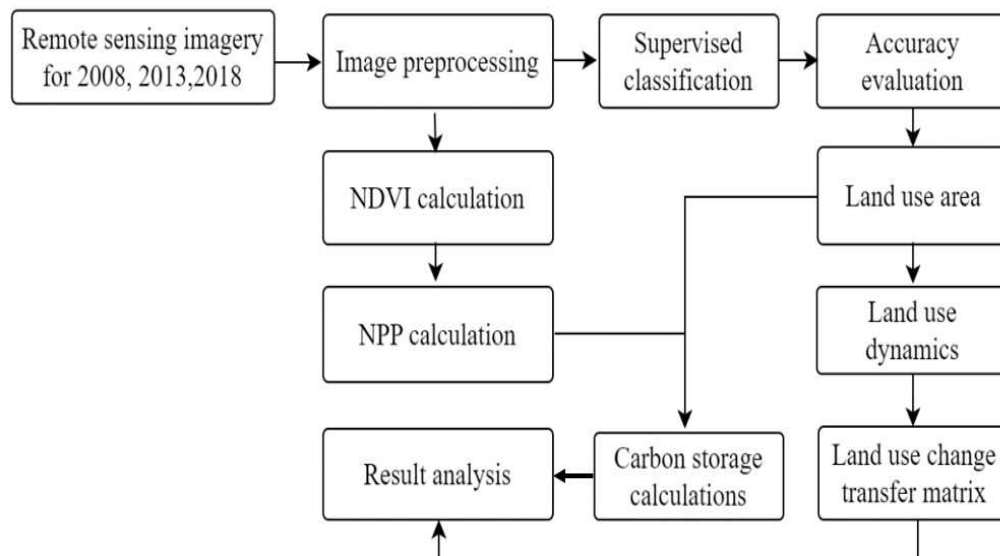


Figure 1: The Map of Shenzhen Administrative Division.

## Methods

Determine the technical process of the research according to the main contents and methods of the research, hence this study proposes a processing framework (the technical framework shows Figure 2). The technical route is divided into four parts: such as data acquisition and preprocessing, classification of LULC types (including the land type transfer matrix calculation), NPP calculation as well as green space carbon storage calculation.

- Data acquisition and preprocessing. The data in this study is using Landsat-8 satellite series data and meteorological data. The RS data are preprocessed by clipping, radiometric calibration, atmospheric correction and mosaic, and the solar radiation data are calculated by using the empirical model. Then, extracted the NDVI, Ratio vegetation index (SR), FPAR and APAR to preparing for the NPP of Vegetation calculation.
- Classification of LULC types. Based on multi-source RS data fusion, the SVM classification method is used to classify the study area, and proving by kappa value, extract the regional LULC data, and then calculate the regional LULC dynamic degree as well as calculate the land type transfer matrix.
- NPP calculation. Based on the classification results of urban LULC types and the results of physical and chemical parameters of vegetation, combined with meteorological data and the maximum solar energy utilization rate of vegetation, the CASA estimation model is established to realize the estimation of NPP.
- Green space carbon storage calculation. Incorporation with NPP and LULC area data that were used to calculate the carbon storage of green space in Shenzhen.



**Figure 2: The Framework of Process Methods.**

### Data Source and Processing

The RS images used in this study are downloaded from the free imagery website which is provided by Geospatial Data Cloud (GDC). Landsat-8 images were downloaded in 2013 and 2018, but without landsat-8 images were available in 2008, so Landsat-5 images were used. The relevant data is shown in Table 1.

**Table 1: Metadata of Satellite Images used in this Research**

Year	Satellite	Sensor	Original Bands Numbers	Pixel Resolution	Path/Row
2008	Landsat-5	TM	1,2,3,4,5,7	30m	121/044 122/044
2013	Landsat-8	OLI	1,2,3,4,5,7,8	30m	122/044
2018	Landsat-8	OLI	1,2,3,4,5,7,8	30m	122/044

This study uses ENVI 5.3 software to carry out a serial of process such as radiometric calibration, atmospheric correction, image mosaic and clipping for the images of the three periods respectively. The atmospheric corrected images are extracted, and the NDVI is calculated by near infrared (NIR) wavelength and red light band (R). Generally, the calculate expressions are used as follows:  $NDVI = \frac{NIR - R}{NIR + R}$  (Liou et al., 2021; Gouzile et al., 2022).

Additionally, the NPP calculation involves solar radiation data. According to the existing empirical formula of total solar radiation (Du et al., 2003; Zhou et al., 2022), such as the solar radiation data of Shenzhen is calculated:  $Q = Q_0(a + bs)$  Where  $Q_0$  is the total astronomical, radiation  $a, b$  are the empirical coefficients, and  $s$  is the percentage of sunshine. The sunshine hours are from the statistical yearbook of Shenzhen.

### Dynamic Degree of LULC

LULC dynamics usually can describe the intensity of land change in a certain period of time and predict the trend of LULC change. The expressions are described as formula (1) (Li et al., 2021).

$$K = \frac{U_b - U_a}{U_a} \times \frac{1}{T} \times 100\% \quad (1)$$

Where:  $K$  is the dynamic degree of single LULC type in time; The interval is  $T$ ;  $U_a$  is the initial area of a land type study;  $U_b$  is the area at the end of a land study. A positive value of  $K$  indicates an increase in land area and a negative value indicates a decrease in land area.

### Classification Method and Accuracy Evaluation

Using ENVI software, fully considering the LULC characteristics of Shenzhen and referring to the land classification method of Maitiniyazi and Kasimu (2018), the LULC types of the study area are combined into five first-class LULC units, as shown in Table2, namely green space, water areas, cultivated land, construction land and unused land (Fatima and Javed, 2021), and then the SVM method used to supervise the classification to obtain the LULC data of Shenzhen.

**Table 2: The Classification of LULC Coverage/Utilization in Shenzhen**

Primary Classification	Secondary Classification
Construction land	Town
	Traffic land
	Settlements
	Industrial and mining land
Water areas	Reservoir
	Lakes
Green space	Woodland
	Grassland
Cultivated land	Farmland
Unused land	Bare ground
	Other lands

Visual interpretation is used to verify the accuracy of supervision and classification results in Shenzhen, and the overall accuracy is more than 90%. In this study, the overall classification accuracy and kappa coefficient are used to evaluate the accuracy of LULC classification results. The overall classification accuracy is equal to the sum of correctly classified pixels divided by the total number of pixels. The value of kappa coefficient indicates: 0.0-0.20 extremely low consistency, 0.21-0.40 general consistency, 0.41-0.60 medium consistency, 0.61-0.80 high consistency and 0.81-1 almost completely consistent.

## NPP Calculation

As an important part of surface carbon cycle, NPP is the main factor to determine ecosystem carbon sink. In the study of the impact of global change on the ecosystem, NPP has become an indispensable index (Tang et al., 2013). The principle of RS technology in carbon sequestration research is to calculate the relationship between absorbed radiation and primary productivity by recording the spectral response of plants during photosynthesis with sensors, so as to obtain NPP, and then estimate the carbon sequestration capacity of plants. According to the mechanism and structure of the model, the commonly used NPP estimation methods can be divided into three types: statistical model, light energy utilization model and process model. Based on the data of land classification results, in this study the improved CASA model is used to estimate the NPP of Shenzhen, gradually calculate NDVI, SR, FPAR and APAR, and finally calculate the NPP. The calculation process is as follows:

### (1) Normalized Vegetation Index (NDVI)

In 1973, NDVI was proposed to observe the amount of vegetation on the earth's surface, which has become a widespread and practical method so far. The principle is that chlorophylls in plants has a large amount of absorption of red light (R) and strong reflection of near-infrared light (NIR). NDVI can be used to observe the vegetation cover of land. The closer NDVI is to 1, the higher the vegetation density is; the closer to 0, the lower the planting density. That is, the vegetation leaf surface has strong absorption characteristics in the visible red light band and strong reflection characteristics in the near-infrared band, which is the physical basis of quantitative RS monitoring of vegetation index (Liou et al., 2021; Gouzile et al., 2022; Zhou et al., 2022).

Vegetation Index (VI) is a quantitative radiation value that reflects the relative abundance and activity of green living vegetation. It is often used to characterize the physiological status of vegetation, green biomass and vegetation productivity in the study area. At present, more than 20 kinds of VI have been proposed, such as Ratio Vegetation Index (RVI), Difference Vegetation Index (DVI), Normalized Difference Vegetation Index (NDVI), Enhanced Vegetation Index (EVI), Perpendicular Vegetation Index (PVI), Soil-Adjusted Vegetation Index (SAVI), Modified Soil Adjustment Vegetation Index (MSAVI), etc. Among them, the NDVI is the most widely used. The formula (2) for calculating this index is:

$$NDVI = \frac{NIR-R}{NIR+R} \quad (2)$$

Where the NDVI range is [- 1, 1]. It is calculated by near infrared wavelength and red light band.

### (2) Ratio Vegetation Index (SR)

The characteristics of plants reflecting and absorbing infrared light are used to reflect the richness of plants. However, this index will have large errors due to regional and seasonal differences, so it is impossible to directly use this index to compare the relative relationship of image planting in different regions or at different times. Represented by formula (3):

$$SR_{(x,t)} = \frac{1+NDVI_{(x,t)}}{1-NDVI_{(x,t)}} \quad (3)$$

Where NDVI (x, t) represents the NDVI value of pixel x in period t, which is calculated by the formula.

### (3) Fraction of Photosynthetically Active Radiation (FPAR)

The FPAR refers to the effective radiation of photosynthesis incident above the vegetation canopy, that is, the absorption ratio of PAR (Photosynthetically Active Radiation) received by the vegetation canopy. Its calculation method is as follows: The maximum values ( $NDVI_{max}$ ,  $SR_{max}$ ) and minimum values ( $NDVI_{min}$ ,  $SR_{min}$ ) of NDVI and SR of vegetation types are calculated respectively through the cumulative frequency of 95% and 5%. Within a certain range, there is a linear relationship between FPAR and NDVI. FPAR can be determined according to the maximum and minimum values of NDVI of vegetation and the corresponding maximum and minimum values of FPAR (Zhu et al., 2006).

The values of  $FPAR_{max}$  and  $FPAR_{min}$  are independent of vegetation type. 5% NDVI value represents desert and bare land, and 95% NDVI value represents that the vegetation is in full coverage. At this time, the corresponding  $FPAR_{max}$  is 0.95; 5% NDVI value represents bare ground, and its corresponding  $FPAR_{min}$  is 0.001 (Zhu et al., 2006), which is expressed by formula (4):

$$FPAR_{NDVI} = \frac{NDVI(x,t) - NDVI(i,min)}{NDVI(i,max) - NDVI(i,min)} \times (FPAR_{max} - FPAR_{min}) + FPAR_{min} \quad (4)$$

The research shows that there is also a linear relationship between FPAR and ratio vegetation index (SR) (Zhu et al., 2006), which is expressed by (5):

$$FPAR_{SR} = \frac{SR(x,t) - SR(i,min)}{SR(i,max) - SR(i,min)} \times (FPAR_{max} - FPAR_{min}) + FPAR_{min} \quad (5)$$

In order to minimize the error, the study combines the FPAR estimated by NDVI and the FPAR estimated by SR, and takes the average value as the estimated value of FPAR. Since the non-vegetated area has NDVI value, the FPAR is calculated by region according to the current land classification situation of Shenzhen,  $\alpha$  is the adjustment coefficient between the two methods. Take the average value of 0.5 (Maitiniyazi and Kasimu, 2018) and combine equation (4) and equation (5) to obtain equation (6):

$$FPAR(x, t) = \begin{cases} 0 & \text{Construction land} \\ \alpha FPAR_{NDVI} + (1 - \alpha) FPAR_{SR} & \text{Green space} \end{cases} \quad (6)$$

### (4) Absorbed Photosynthetically Active Radiation (APAR)

The APAR refers to the proportion of photosynthetic effective radiation absorbed by vegetation in the total solar radiation, which reflects the strength of photosynthesis of vegetation, and the carbon sequestration capacity of vegetation. The light and effective radiation of vegetation depends on the total solar radiation and the characteristics of the plant itself (Jiao et al., 2020). Represented by equation (7):

$$APAR(x, t) = SOL(x, t) \times FPAR(x, t) \times 0.5 \quad (7)$$

In formula (7),  $APAR(x, t)$  is the Photosynthetic active radiation ( $MJ \cdot m^{-2} \cdot t^{-1}$ ) absorbed by the vegetation in pixel  $x$  in time period  $t$ ;  $SOL(x, t)$  is the total solar radiation ( $MJ \cdot m^{-2} \cdot t^{-1}$ ) received by pixel  $x$  in time period  $t$ , which is calculated by empirical formula (Du et al., 2003);  $FPAR(x, t)$  is the proportion of photosynthetic effective radiation absorption of vegetation in pixels; 0.5 represents the proportion of total solar radiation used for photosynthesis.

### (5) NPP of Vegetation Calculation

NPP of vegetation can be absorbed by plants, APAR and actual light utilization( $\varepsilon$ ) expressed by two factors, the unit is ( $\text{g C}\cdot\text{m}^2$ ):

$$NPP(x, t) = APAR(x, t) \times \varepsilon(x, t) \quad (8)$$

$\varepsilon(x, t)$ , represents the actual light energy utilization of pixel  $x$  in month  $t$ .

### Carbon Storage Calculation

The following vegetation carbon sequestration model (Wang and Gu, 2012; Zhou et al., 2022) is mainly used to estimate the carbon storage of vegetation in the study area, which is estimated by the area of different land cover, NPP of vegetation and carbon conversion coefficient of different vegetation:

$$E = T \times \delta \times c \quad (9)$$

Where,  $E$  represents the carbon sequestration amount of land cover type ( $\text{kg}$ );  $T$  refers to the land area ( $\text{m}^2$ ) corresponding to the land cover type;  $\delta$  represents the **NPP** of land cover type ( $\text{gC}\cdot\text{m}^2$ );  $c$  means the conversion factor between vegetation biomass and carbon content is 0.45 (Wang and Gu, 2012).

### ANALYSIS OF LULC CHANGE

In this chapter, the spatial-temporal change analysis, dynamic degree analysis and transfer matrix analysis of LULC in the study area will be carried out respectively (Zhao and Du, 2022). Before this analysis process, RS images must be classified first, but the accuracy of classification is generally evaluated by kappa value. Finally, the kappa coefficient of the supervised classification results is above 0.90, indicated that with high accuracy. The results are shown in Table 3:

**Table 3: The Results of the Classification Accuracy Evaluation**

	2008	2013	2018
Accuracy Assessment	96.63%	96.46%	92.89%
Kappa	0.95	0.95	0.90

### Analysis of Spatial-Temporal Change of LULC

The supervised classification method selects the SVM to obtain the LULC data of Shenzhen in three periods, and then carries out classification statistics to obtain the spatial distribution area and area of various LULC types (as shown in Figure 3, Figure 4, Figure 5 and Table 4). In order to more intuitively unfold the LULC change in the study area, the LULC change area and LULC dynamic degree in Shenzhen were calculated.

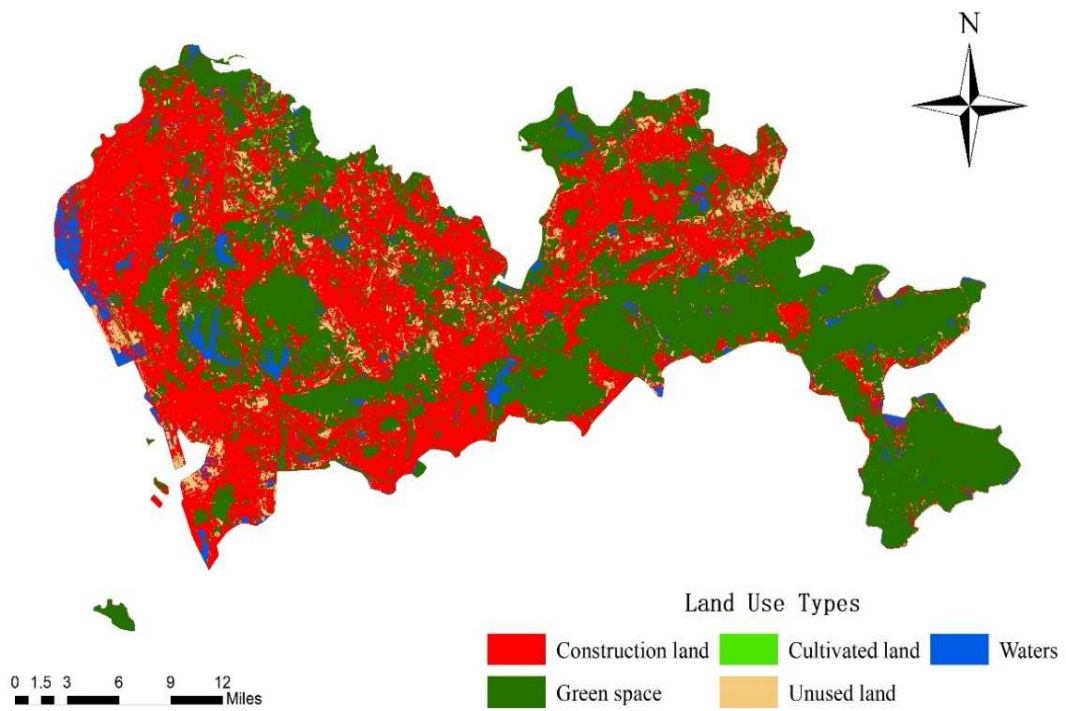


Figure 3: The LULC Map of Shenzhen in 2008.

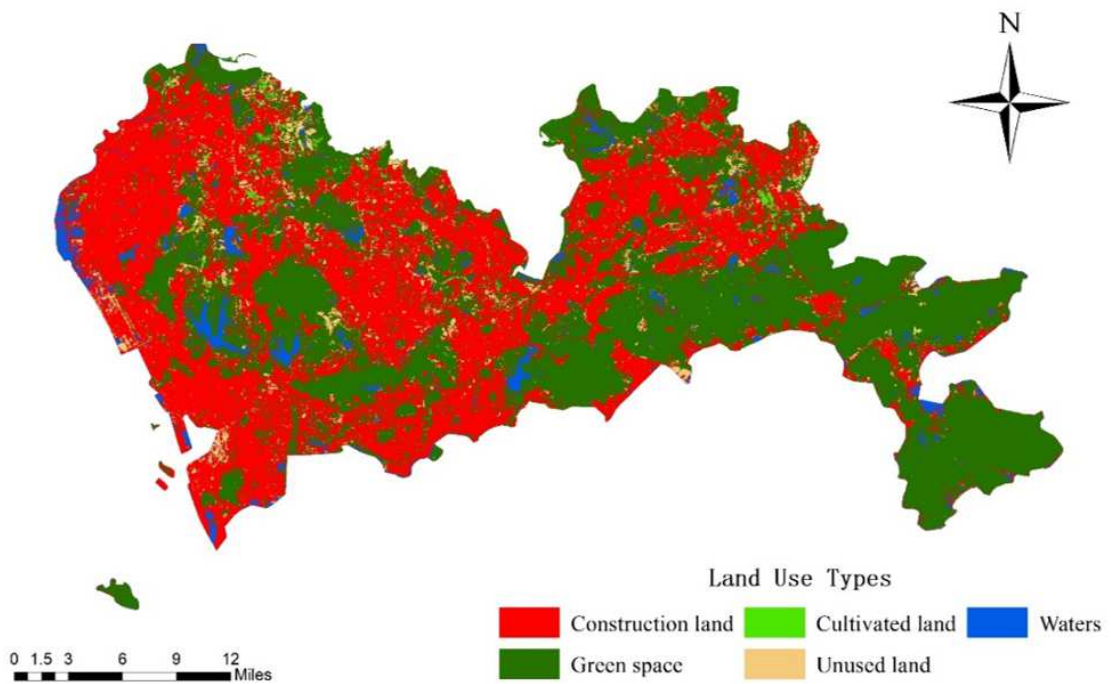


Figure 4: The LULC Map of Shenzhen in 2013.

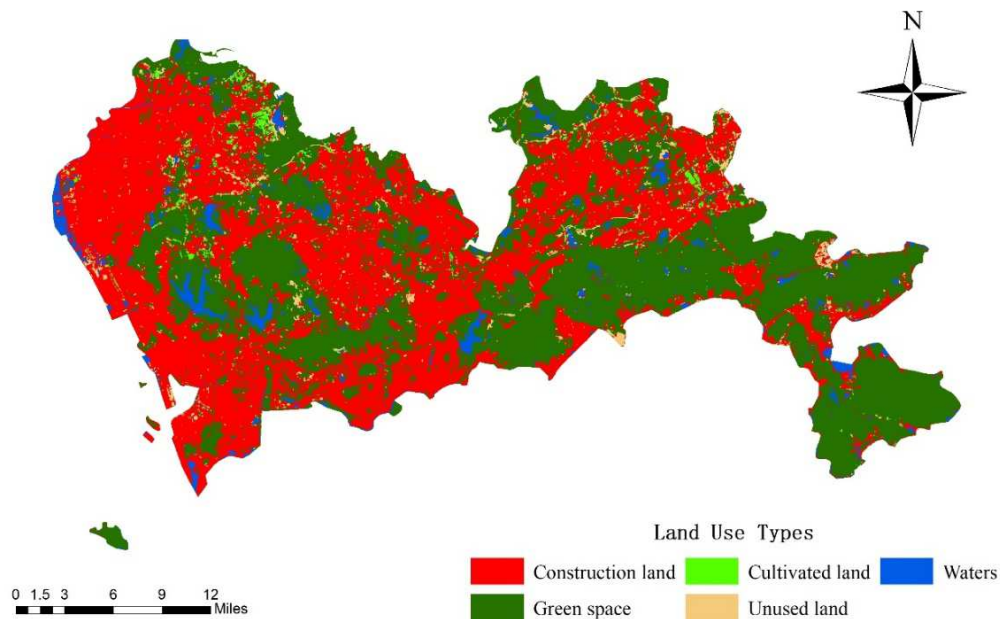


Figure 5: The LULC Map of Shenzhen in 2018.

Table 4: The Area of LULC Change in Shenzhen from 2008 to 2018 (unit:  $\text{hm}^2$ )

Land Type	2008		2013		2018	
	Area	Proportion	Area	Proportion	Area	Proportion
Construction Land	85490.7	43.8%	89056.0	45.6%	91886.2	47.0%
Green Space	91677.6	46.9%	89531.3	45.8%	89178.4	45.6%
Cultivated Land	2161	1.1%	3384.9	1.7%	2496.3	1.3%
Water Areas	6997.5	3.6%	6925.3	3.5%	4854.2	2.5%
Unused Land	9039.1	4.6%	6468.4	3.3%	6950.7	3.6%
Total	195365.9	100.0%	195365.9	100.0%	195365.9	100.0%

It can be found that the LULC types in Shenzhen are mainly construction land and green space, followed by water areas and unused land, and the cultivated land is the least (shown as Table 4). In 2018, for example, the construction land and green space area reached  $91886.2 \text{ hm}^2$  and  $89178.4 \text{ hm}^2$ , accounting for 47.0% and 45.6% respectively, while the total proportion of cultivated land, water areas and unused land was only 7.6%.

From 2008 to 2018, the construction land in Shenzhen increased by  $6395.5 \text{ hm}^2$ . As a carbon source, the construction of land is one of the important factors affecting carbon emissions. The vegetation is reduced, and the solidification effect of vegetation on carbon in the air is greatly weakened. Meanwhile, vegetation residues will also emit a large amount of carbon, and the solidification effect of soil on carbon will also be weakened, resulting in an increase in carbon emissions. From 2008 to 2013, the green area decreased steadily by  $2146.3 \text{ hm}^2$ , 2013 to 2018, which showed that Shenzhen attached importance to urban greening and low-carbon development.

The cultivated land area increased slightly from 2008 to 2013, increased by  $1223.9 \text{ hm}^2$ , and decreased in 2018. The increase of urban population, rapid economic development and industrial structure adjustment are important reasons for the decrease of cultivated land. The water areas has decreased year by year, indicating that the development of urbanization has eroded a large number of water areas, which is not conducive to environmental protection in Shenzhen. The unused land showed a downward trend from 2008 to 2013 and increased in 2018, indicating that the land supply and demand in Shenzhen is tight, and the unused land is gradually developed for construction or other purposes.

### Dynamic Degree Analysis of LULC

The single LULC dynamic degree mainly represents the change degree of a certain land type in a certain region. The dynamic degree of single LULC of Shenzhen in 2008-2013, 2013-2018 and 2008-2018 is calculated from equation (1). The results are shown in Table 5.

**Table 5: The Dynamics Degree of Single LULC in Shenzhen**

Land Type	2008-2013	2013-2018	2008-2018
Construction Land	0.0083%	0.0064%	0.0075%
Green Space	-0.0047%	-0.0008%	-0.0027%
Cultivated Land	0.1133%	-0.0525%	0.0155%
Water Areas	-0.0021%	-0.0598%	-0.0306%
Unused Land	-0.0569%	0.0149%	-0.0231%

It can be seen from Table 5 that during 2008-2018, cultivated land and construction land increased at the rate of 0.0155% and 0.0075% respectively, while green space, water areas and unused land decreased at the rate of 0.0027%, 0.0306% and 0.0231% respectively. The area of construction land increases year by year, with a rapid increase rate. The increase rate from 2008 to 2013 is faster than that from 2013 to 2018. The area of green space decreases year by year, but the reduction rate decreases from 0.0047% to 0.0008%. The single dynamic degree of the water areas decreased from 0.0021% to 0.0598%. The reduction of the water areas will have an adverse impact on the ecological environment of Shenzhen. The rate of unused land has changed from decrease to increase, indicating that Shenzhen will develop other types of land to increase LULC.

### Analysis of LULC Transfer Matrix

Applying the LULC area transfer matrix to quantitatively analyze the change direction of different land types and understand the evolution process of land types in the study area. It can be seen from Table 6 and Table 7 that the LULC change in Shenzhen during the two periods showed the characteristics of one land type changing to a variety of other types.

**Table 6: The LULC Type Transfer Matrix from 2008 to 2013 (unit: hm<sup>2</sup>)**

2008	2013					
	Construction Land	Green Space	Cultivated Land	Water Areas	Unused Land	Total
Construction Land	72484.4	8696.8	1162.5	1605.6	1541.4	85490.7
Green Space	10207.9	76392.2	2014.8	2065.7	996.9	91677.5
Cultivated Land	897.1	815.4	262.6	150.8	35.2	2161.1
Water Areas	5906.6	1696.2	473.5	857.7	105.2	9039.2
Unused Land	1351.2	341.7	81.4	322.4	4900.8	6997.5
Total	90847.2	87942.3	3994.8	5002.2	7579.5	195365.9

From 2008 to 2013, green space was the main type of transfer out, with a total of 15285.3hm<sup>2</sup> transferred out, of which the area converted to construction land was the largest, accounting for 67.8% of the total transferred out area; Secondly, it is transformed into water areas and farmland. The decomposition of organic soil will be accelerated in the process of farmland cultivation, so the conversion from forest to farmland will lead to the release of greenhouse gases such as carbon dioxide from the terrestrial biosphere to the atmosphere. The construction land is mainly converted into green space, with 8696.8hm<sup>2</sup> transferred out. The withdrawal of construction land reclamation will increase the green area, which will increase regional carbon storage to a certain extent. The 897.1hm<sup>2</sup> of cultivated land is converted into construction land and 815.4hm<sup>2</sup> into green space. Cultivated land can be regarded as carbon sink to some extent. On the whole, good soil can store more carbon than release.

**Table 7: The LULC Type Transfer Matrix from 2013 to 2018 (unit: hm<sup>2</sup>)**

2013	2018					
	Construction Land	Green Space	Cultivated Land	Water Areas	Unused Land	Total
Construction Land	80150.8	6032.2	460.9	1341.4	1070.7	89056.0
Green Space	6218.8	80460.6	779.6	1717.4	355.0	89531.3
Cultivated Land	1135.4	1067.0	826.0	304.6	51.8	3384.9
Water Areas	3459.0	1140.0	403.9	1323.0	142.4	6468.3
Unused Land	922.3	478.7	25.9	167.8	5330.8	6925.4
Total	91886.2	89178.4	2496.3	4854.2	6950.7	195365.9

From 2013 to 2018, construction land and green space were still the main transfer out types. Due to population growth, transportation and housing will inevitably occupy a certain green space area. However, compared with 2008-2013, the transfer out area of green space decreased, indicating that Shenzhen attaches importance to protecting the ecological environment, and vigorously carries out to build the forest, to create a garden city, and strives to achieve the "National Forest City". Secondly, the conversion of cultivated land to construction land and green space is a positive ecological evolution process, which can significantly increase the carbon sink function of terrestrial ecosystem, which is also related to the implementation of the national policy of returning cultivated land to forest. Additionally, the water areas are mainly transformed into construction land.

With the rapid development of Shenzhen, the transfer of construction land has gradually increased. Cultivated land, green space and unused land are the main sources of construction land. During this period, woodland has been transformed into cultivated land. It can be seen that before 2013, Shenzhen was mainly in a high-speed development period. In the process of urban construction, the demand for construction land is increasing, the scale of carbon source land is increasing, and the growth rate of construction land is large, it should lead to an increase in carbon emissions, and the forest land with high carbon sink is losing.

## **NPP AND CARBON STORAGE ANALYSIS**

### **NPP Analysis**

According to the analysis and calculation of this study (as shown in Figure 6, Figure 7 and Figure 8), the maximum NPP of Shenzhen in 2008 was 160.6 g C·m<sup>-2</sup>, the maximum value in 2013 was 134.0 g C·m<sup>-2</sup> and the maximum value in 2018 was 134.4 g C·m<sup>-2</sup>, showing the characteristics of high in the eastern mountainous areas and low in the central and western regions. Based on the analysis of the LULC classification map, the green space is mainly distributed in the economically backward southeast region, and the eastern region is mainly forest or mountainous region, with abundant vegetation types and relatively high vegetation NPP. The central and western regions have rapid economic development, frequent human activities, dense urban distribution, relatively small green space distribution and low vegetation coverage, so the NPP of vegetation is low.

In the decade from 2008 to 2018, the NPP first decreased and then increased. From 2008 to 2013, Shenzhen was in the stage of rapid development. Obviously, construction land occupied a large amount of green space and destroyed the surface vegetation coverage, resulting in the decline of NPP. From 2013 to 2018, urbanization accelerated, a large amount of cultivated land was occupied, and the cultivated land area decreased. However, as can be seen from Figure 7 and Figure

8, the NPP value of construction land in 2018 increased significantly compared with that in 2013. The reason is, during this period, Shenzhen also strengthened ecological construction, and increased the construction of road green space and park green space, resulting in an increase in the green area of Shenzhen. Thus, in 2018 Shenzhen won the title of "National Forest City". However, due to urban expansion, part of the green space was converted into construction land, so the NPP value changed slightly.

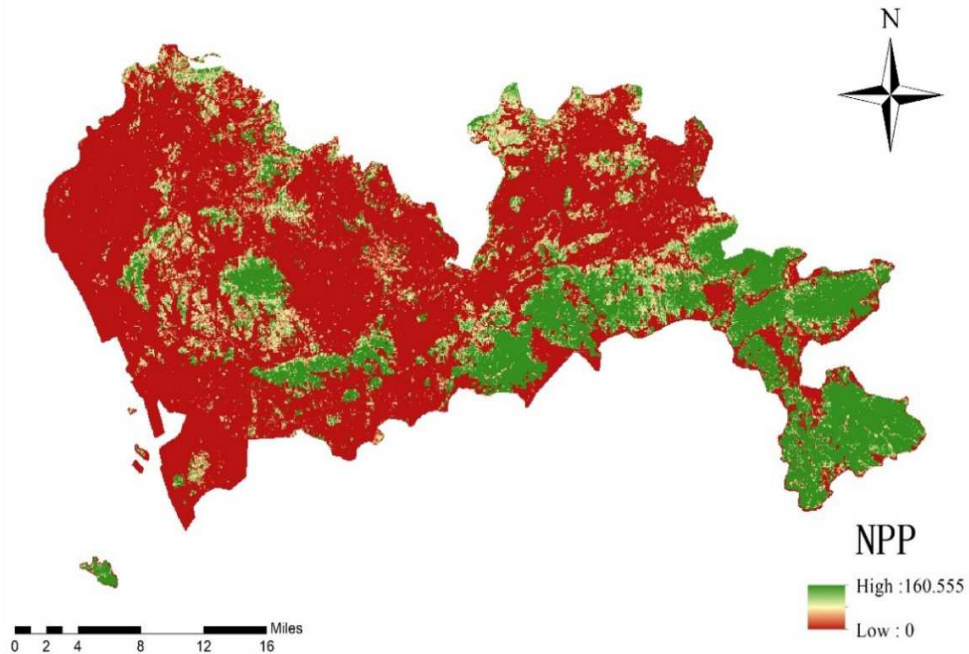


Figure 6: The NPP Distribution Map of Shenzhen in 2008.

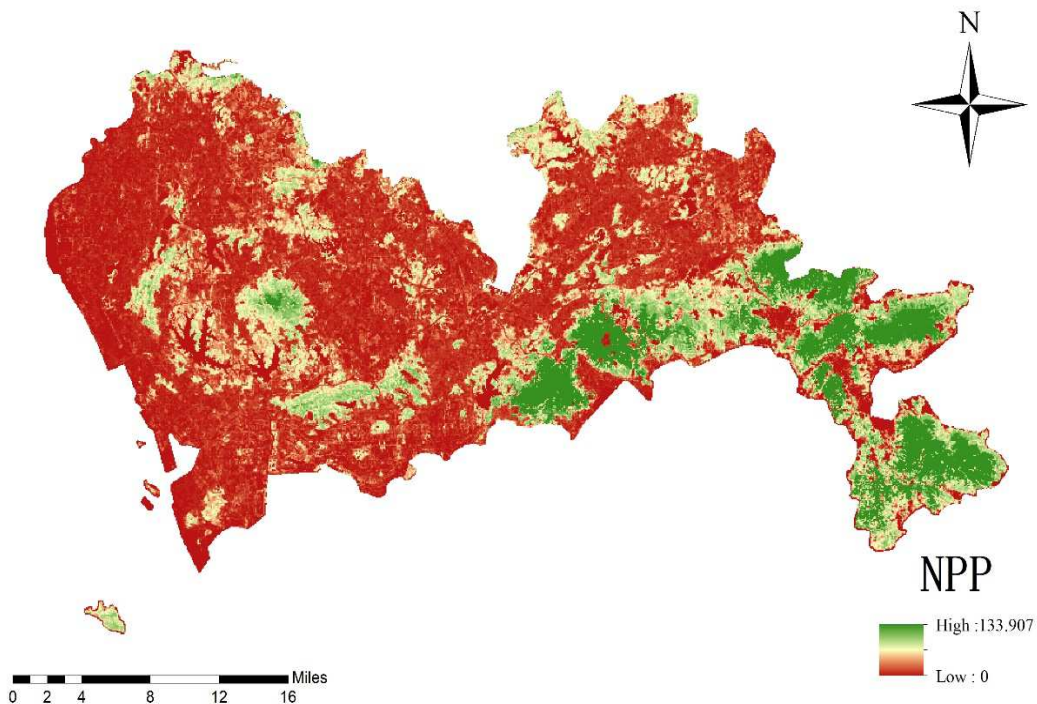
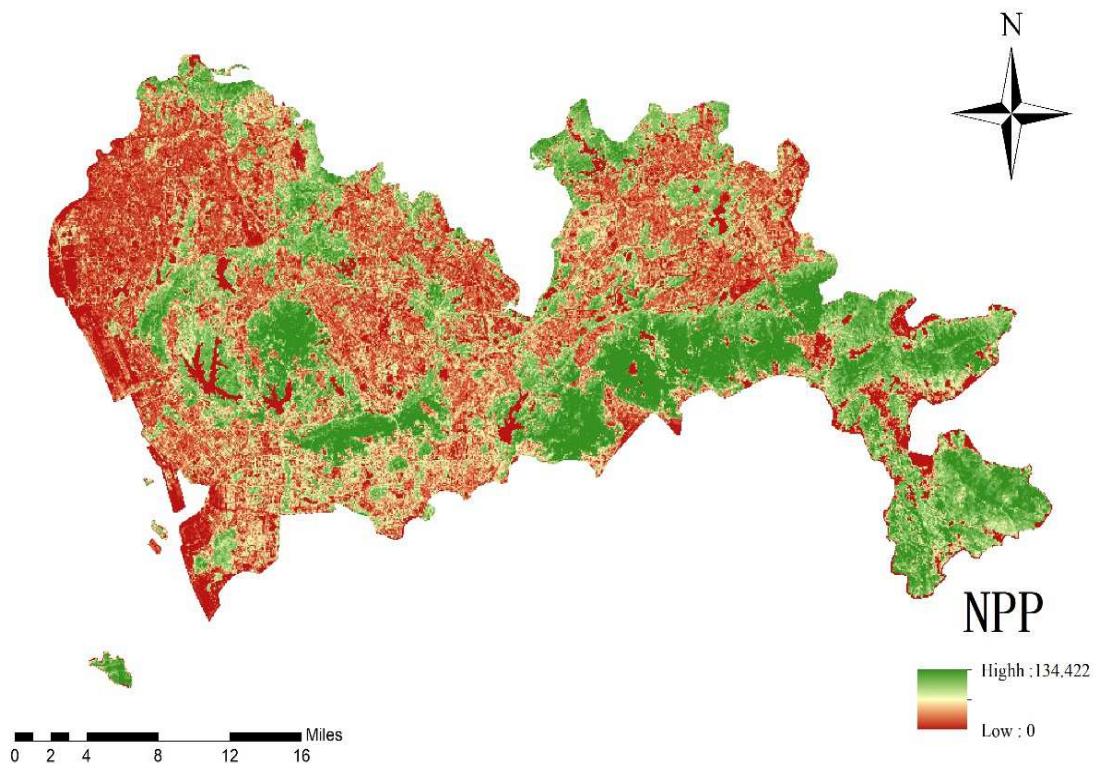


Figure 7: The NPP Distribution Map of Shenzhen in 2013.



**Figure 8: The NPP Distribution Map of Shenzhen in 2018.**

### Carbon Storage Analysis

According to formula (9), the calculation of carbon storage of green field in Shenzhen in 2008, 2013 and 2018 was  $4.26 \times 10^6$  t,  $3.58 \times 10^6$  t,  $4.2 \times 10^6$  t respectively. The results are shown in Table 8.

**Table 8: The Carbon Storage of Shenzhen in the Period 2008, 2013 and 2018**

	2008	2013	2018
Green area (hm <sup>2</sup> )	91677.6	89531.3	89178.4
Greenland average NPP (g C·m <sup>2</sup> )	102.88	88.8	106.99
Greenfield carbon storage (t)	$4.26 \times 10^6$	$3.58 \times 10^6$	$4.2 \times 10^6$

The results show that the change of carbon storage of green space in Shenzhen first decreased and then increased. From 2008 to 2013, the change of LULC in Shenzhen led to the decrease of carbon storage of urban green space. During this period, the carbon sequestration capacity of urban ecosystem vegetation weakened. The main reason is that the green space with the highest carbon sequestration capacity was transformed into other types of land, and the green space area was transferred out by 15285.3 hm<sup>2</sup>. The decrease of the green space area led to a decrease in carbon storage of vegetation. However, from 2013 to 2018 the carbon reserves of urban green space are increasing, it is due to the fact that after 2012 the state has vigorously promoted the construction of ecological civilization and focused on promoting green development, sustainability development and low-carbon development. Driven by policies, the urban development in central and western regions of Shenzhen has gradually realized the transformation to green development.

With the continuous expansion of urban construction in Shenzhen, the contradiction between land-use is prominent, and the high density of population and buildings makes the ecological environment face severe challenges. Therefore, Shenzhen has promoted a policy of "three-dimensional greening", which peculiar ideas has "borrow land" from

roofs, walls, three-dimensional bridges, etc., and build greening in the air. This policy may also be one of the important factors affecting the change of carbon reserves of urban green space in Shenzhen. In this context, the ecological benefits of Shenzhen have been raised to a new level.

## CONCLUSIONS

Based on the LULC change and NPP calculation of vegetation, this study estimates the carbon storage in Shenzhen and analyzes the change of carbon storage. The results show that:

- During the period 2008-2013, the regional LULC type changes have obvious differences. Construction land increased by 3565.3hm<sup>2</sup>, cultivated land increased by 1223.9hm<sup>22</sup>, and green space decreased by 2146.3hm. Among them, the decreased green space is mainly transferred out as construction land, and cultivated lands as well as construction land are mainly transferred in. Thus, that kind of change we realize which resulting in the decrease of vegetation may also lead to the decrease of vegetation carbon storage, indicating that the carbon storage capacity of vegetation in Shenzhen was generally weakened during this period.
- From 2013 to 2018, the difference of LULC types is not obvious, the change range of green space area is small, however the area of construction land is still increasing, so that the green space, and cultivated land, water areas as well as unused land are converted to construction land. Nevertheless, during this period, the NPP of urban green space showed an upward trend, meanwhile carbon reserves is increased by 0.95 compared with 2013 of 106 tons, which may have a certain relationship with returning farmland to forest and green policy development.

From the perspective of above analysis results, this study adopts the combination of RS and GIS technology to analyze the land transfer of land environmental changes in Shenzhen in recent decade, as well as calculating the NPP of green space and carbon storage, which can effectively obtain the environmental monitoring benefits of the study area. Meanwhile, it can obtain further empirical proof according to the comparative evaluation of Shenzhen's environmental policies. Therefore, the experimental proof and contribution significance of this study have two crucial perspectives. Firstly, in terms of technical analysis, verify the feasibility and rationality of RS and GIS technology, as well as the availability and contribution in the long-term environmental perception monitoring in the future. Secondly, in terms of the practice of policy and decision-making, this study proves the effectiveness and contribution of urban greening, provides effective proof for the continuous promotion of the "dual carbon" policy in near future, and has a better empirical tool on the road of sustainable development.

Therefore, to achieve the goal of "Carbon Peak and Carbon Neutralization", we should vigorously develop urban greening, increase urban green vegetation, restore and protect forest, wetland, marine and other ecosystems, and increase the capacity of land and marine carbon sinks. In recent years, there have obvious implementing effectiveness on Shenzhen, that has actively built urban greenways, community greenways and regional greenways, and built a three-level park construction system of "Natural Park, Urban Park, Community Park", so as to form a green environment pattern with good ecology, beautiful landscape, distinctive characteristics and harmonious development between man and nature, and contribute to the realization of the environmental carbon neutral vision.

Overall, the monitoring and analysis data of this study show that good greening policies and actions can indeed achieve the purpose of environmental improvement and provide feasible thinking for the realization of the "dual carbon" goal.

## ACKNOWLEDGEMENTS

The author is grateful for the research grants given to Ruei-Yuan Wang from GDUPT Talents Recruitment (NO. 2019rc098), Peoples R China under Grant No. 702-519208, and Academic Affairs in GDUPT for Goal Problem-Oriented Teaching Innovation and Practice Project Grant No. 701-234660.

## CONFLICTS OF INTEREST

The authors declare no conflicts of interest regarding the publication of this paper.

## REFERENCES

1. Aka, K.; Dibi, H.; Koffi, J.; Bohoussou, C. *Land Cover Dynamics and Assessment of the Impacts of Agricultural Pressures on Wetlands Based on Earth Observation Data: Case of the Azagny Ramsar Site in Southern Côte d'Ivoire*. *Journal of Geoscience and Environment Protection*, 2022, 10, 43-61. doi: 10.4236/gep.2022.105004.
2. Amraoui, M.; Kabiri, L.; Kassou, A.; Ouali, L.; Nutz, A. *Diachronic Study of the Vegetation Covers Spatiotemporal Change Using GIS and Remote Sensing in the Ferkla Oasis: Case Study, Bour El Khourbat, Tinjdad, Morocco*. *Journal of Geoscience and Environment Protection*, 2022, 10, 173-188. doi: 10.4236/gep.2022.101012.
3. Bonneuil, C.; Choquet, P.L.; Franta, B. *Early warnings and emerging accountability: Total's responses to global warming, 1971–2021*. *Global Environmental Change*, 2021, 71, 102386. <https://doi.org/10.1016/j.gloenvcha.2021.102386>
4. Bordoloi, R.; Das, B.; Tripathi, O.P.; Sahoo, U.K.; Nath, A.J.; Deb, S.; Das, D.J.; Gupta, A.; Devi, N.B.; Charturvedi, S.S.; Tiwari, B.K.; Paul, A.; Tajo, L. *Satellite based integrated approaches to modelling spatial carbon stock and carbon sequestration potential of different land uses of Northeast India*. *Environmental and Sustainability Indicators*, 2022, 13, 100166. <https://doi.org/10.1016/j.indic.2021.100166>
5. Byomkesh, T.; Nakagoshi, N.; Dewan, A. M. *Urbanization and green space dynamics in Greater Dhaka, Bangladesh*, 2012, 8(1), 45–58. <https://doi.org/10.1007/s11355-010-0147-7>
6. Chen, Y.N. *Multiple Kernel Feature Line Embedding for Hyperspectral Image Classification*. *Remote Sens.* 2019, 11, 2892. <https://doi.org/10.3390/rs11242892>
7. Chen, C.; Tabssum, N.; Nguyen, H. P. *Study on Ancient Chu Town Urban Green Space Evolution and Ecological and Environmental Benefits*. *Nature Environnement and Pollution Technology*, 2019, 18, 1733-1738.
8. Cheng, M.; McCarl, B.; Fei, C. *Climate Change and Livestock Production: A Literature Review*. *Atmosphere* 2022, 13, 140. <https://doi.org/10.3390/atmos13010140>
9. Choudhury, D.; Nath, D.; Chen, W. *Near Future Projection of Indian Summer Monsoon Circulation under 1.5 °C and 2.0 °C Warming*. *Atmosphere* 2022, 13, 1081. <https://doi.org/10.3390/atmos13071081>
10. Dan-jumbo, N. G.; Metzger, M. J.; Clark, A. P. *Urban Land-Use Dynamics in the Niger Delta: The Case of Greater Port Harcourt Watershed*. *Urban Science*, 2018, 2, 108. <https://doi.org/10.3390/urbansci2040108>

11. Deng, O.; Li, Y.; Li, R.; Yang, G. Ecosystem Services Evaluation of Karst New Urban Areas Based on Net Primary Productivity of Guanshanhu District, Guiyang, Guizhou Province, China. *Open Journal of Ecology*, 2022, 12, 377-390. <https://doi.org/10.4236/oje.2022.126022>
12. Du, Y. D.; Mao, H. Q.; Liu, A. J.; Pan, W. J. The Climatological Calculation and Distributive Character of Global Solar Radiation in Guangdong Province. *Resources Science*, 2003, 25(06), 66-70.
13. Fan, Y.; Wei, F. Contributions of Natural Carbon Sink Capacity and Carbon Neutrality in the Context of Net-Zero Carbon Cities: A Case Study of Hangzhou. *Sustainability*, 2022, 14(5), 2680. <https://doi.org/10.3390/su14052680>.
14. Fatima, N.; Javed, A. Assessment of Land Use Land Cover Change Detection Using Geospatial Techniques in Southeast Rajasthan. *Journal of Geoscience and Environment Protection*, 2021, 9, 299-319. <https://doi.org/10.4236/gep.2021.912018>.
15. Field, C. B.; Randerson, J. T.; Malmström, C. M. Global net primary production: Combining ecology and remote sensing, 1995, 51(1), 74–88. [https://doi.org/10.1016/0034-4257\(94\)00066-v](https://doi.org/10.1016/0034-4257(94)00066-v)
16. Guan, D.; Chen, Y.; Huang, X. Carbon storage, distribution and its role in carbon and oxygen balance in Guangzhou urban green space system. *China Environmental Science*, 1998, 18(5), 437-441. <https://doi.org/10.3321/j.issn:1000-6923.1998.05.015>
17. Gouzile, A.; Bama, M.; Zamina, B.; Yapi, E.; Soro, G.; Goula, B.; Issiaka, T. Mapping of Malaria Risk Related to Climatic and Environmental Factors by Multicriteria Analysis in the Marahoué Region of Côte d'Ivoire. *Journal of Geoscience and Environment Protection*, 2022, 10, 234-252. <https://doi.org/10.4236/gep.2022.106015>.
18. Han, H.; Gao, J.; Liu, G. Ecological benefit assessment of urban vegetation by remote sensing and GIS. *Chinese Journal of Applied Ecology*, 2003, 14(12), 2301-2304.
19. Imani, M.; Lo, S.L.; Fakour, H.; Kuo, C.Y.; Mobasser, S. Conceptual Framework for Disaster Management in Coastal Cities Using Climate Change Resilience and Coping Ability. *Atmosphere* 2022, 13, 16. <https://doi.org/10.3390/atmos13010016>
20. Jiao, X.; Zhang, H.; Xu, F.; Wang, Y.; Peng, D.; Li, C.; Xu, X.; Fan, H.; Huang, Y. Analysis of the Spatio-temporal Variation in FPAR of the Tibetan Plateau from 1982 to 2015. *Remote Sensing Technology and Application*, 2020, 35(4), 950-961. <https://doi.org/10.11873/j.issn.1004-0323.2020.4.0950>
21. Jo, H. K.; McPherson, E. G. Carbon storage and flux in urban residential greenspace. *Journal of Environmental Management*, 1995, 45(2), 109~133. <https://doi.org/10.1006/jema.1995.0062>
22. Kashaigili, J.; Mdemu, M.; Nduganda, A.; Mbilinyi, B. "Integrated Assessment of Forest Cover Change and Above-Ground Carbon Stock in Pugu and Kazimzumbwi Forest Reserves, Tanzania," *Advances in Remote Sensing*, 2013, 2(1), 1-9. <https://doi.org/10.4236/ars.2013.21001>.
23. Li, S.; Potter, C.; Hiatt, C. "Monitoring of Net Primary Production in California Rangelands Using Landsat and MODIS Satellite Remote Sensing", *Natural Resources*, 2012, 3(2), 56-65. <https://doi.org/10.4236/nr.2012.32009>.

24. Li, F.; Lu, S.; Li, Y. *Carbon Storage Estimation of Shangri-La Based on CASA Model. Forest Inventory and Planning*, 2015, 40(5), 15–19. <https://doi.org/10.3969/j.issn.1671-3168.2015.05.004>
25. Li, H. *Research advance of forest carbon sink assessment methods and carbon sequestration potential estimation under carbon neutral vision. Geological Survey of China*, 2021, 8(4), 79-86. <https://doi.org/10.19388/j.zgdzdc.2021.04.08>.
26. Li, X.; Lan, L.; Zhu, J.; Xiao, Z. *Analysis of the Dynamic Changes in Land Use and Their Driving Factors in Ganzhou City. Geomatics & Spatial Information Technology*, 2021, 44(02), 24-28.
27. Liou, Y. A.; Kuleshov, Y.; Ho, C. R.; Nguyen, K. A.; Reising, S. C. *Preface: Earth Observations for Environmental Sustainability for the Next Decade. Remote Sens.* 2021, 13, 2871. <https://doi.org/10.3390/rs13152871>
28. Lu, J.; Ren, T.; Yan, D. *Domestic Research on Forest Carbon Sinks. Journal of inner Mongolia Forestry science & Technology*, 2008, 34 (02), 43-47. <https://doi.org/10.3969/j.issn.1007-4066.2008.02.012>
29. Mahamba, J.; Mulondi, G.; Kapiri, M.; Sahani, W. *Land Use and Land Cover Dynamics in the Urban Watershed of Kimemi River (Butembo/D.R.C). Journal of Geoscience and Environment Protection*, 2022, 10, 204-219. <https://doi.org/10.4236/gep.2022.106013>
30. Maitiniyazi, M.; and Kasimu, A. *Spatial-temporal change of Urumqi urban land use and land cover based on grid cell approach. Transactions of the Chinese Society of Agricultural Engineering (Transactions of the CSAE)*, 2018, 34(1), 210-216. <https://doi.org/10.11975/j.issn.1002-6819.2018.01.029>
31. Mirik, M.; Chaudhuri, S.; Surber, B.; Ale, S.; Ansley, R. "Evaluating Biomass of Juniper Trees (*Juniperus pinchotii*) from Imagery-Derived Canopy Area Using the Support Vector Machine Classifier," *Advances in Remote Sensing*, 2013, 2(2), 181-192. <https://doi.org/10.4236/ars.2013.22021>.
32. Myeong, S.; Nowak, D. J.; Duggin, M. J. *A temporal analysis of urban forest carbon storage using remote sensing. Remote Sensing of Environment*, 2006, 101(2), 277-282.
33. Nowak, D. J. *Atmosphere carbon reduction by urban trees. Journal of Environmental Management*, 1993, 37, 207-217. <https://doi.org/10.1006/jema.1993.1017>
34. Peng, X.; Yu, M.; Chen, H. *Projected Changes in Terrestrial Vegetation and Carbon Fluxes under 1.5 °C and 2.0 °C Global Warming. Atmosphere* 2022, 13, 42. <https://doi.org/10.3390/atmos13010042>
35. Piao, S. L.; Fang, J.Y.; Chen, A.P. *Seasonal Dynamics of Terrestrial Net Primary Production in Response to Climate Changes in China. Acta Botanica Sinica*, 2003, 03, 269-275. <https://doi.org/10.3321/j.issn:1672-9072.2003.03.003>
36. Potter, C. S.; Randerson, J.T.; Field, C. B.; Matson, P. A.; Vitousek, P. M.; Mooney, H. A.; Klooster, S. A. *Terrestrial ecosystem production: A process model based on global satellite and surface data. Global Biogeochemical Cycles*, 1993, 7(4), 811–841. <https://doi.org/10.1029/93gb02725>
37. Qian, H.; Ma, R.; Wu, L. *Market-based solution in China to Finance the clean from the dirty. Fundamental Research*, Available online, 2022. <https://doi.org/10.1016/j.fmre.2022.03.020>

38. Quevauviller, P. A Review on Connecting Research, Policies and Networking in the Area of Climate-Related Extreme Events in the EU with Highlights of French Case Studies. *Atmosphere* 2022, 13, 117. <https://doi.org/10.3390/atmos13010117>
39. Rowntree, R. A.; Nowak, D. J. Quantifying the role of urban forests in removing atmospheric carbon dioxide. *Journal of Arboriculture*, 1991, 17(10): 269-275.
40. Shen, J.; Guo, X.; Wan, Y. Identifying and setting the natural spaces priority based on the multi-ecosystem services capacity index. *Ecological Indicators*. 2021, 125: 107473. <https://doi.org/10.1016/j.ecolind.2021.107473>
41. Sun, R.S.; Gao, X.; Deng, L. C.; Wang, C. Is the Paris rulebook sufficient for effective implementation of Paris Agreement? *Advances in Climate Change Research*. Available online, 2022. <https://doi.org/10.1016/j.accre.2022.05.003>
42. Talukdar, S.; Singha, P.; Mahato, S.; Shahfahad; Pal, S.; Liou, Y.-A.; Rahman, A. Land-Use Land-Cover Classification by Machine Learning Classifiers for Satellite Observations—A Review. *Remote Sens*. 2020, 12, 1135. <https://doi.org/10.3390/rs12071135>
43. Tang, J.; Jiang, Y.; Li, Z.Y.; Zhang, N.; Hu, M. Estimation of vegetation net primary productivity and carbon sink in western Jilin province based on CASA model. *Journal of Arid Land Resources and Environment*, 2013, 27(04), 1-7. <https://doi.org/10.13448/j.cnki.jalre.2013.04.026>.
44. Tao, C.; Liao, Z.; Hu, M.; Cheng, B.; Diao, G. Can Industrial Restructuring Improve Urban Air Quality?—A Quasi-Experiment in Beijing during the COVID-19 Pandemic. *Atmosphere* 2022, 13, 119. <https://doi.org/10.3390/atmos13010119>
45. Uwiringiyimana, H.; Choi, J. Remote Sensing and Landscape Metrics-Based Forest Physical Degradation: Two-Decades Assessment in Gishwati-Mukura Biological Corridor in Rwanda, East-Central Africa. *Journal of Geoscience and Environment Protection*, 2022, 10, 64-81. <https://doi.org/10.4236/gep.2022.104005>.
46. Xiong, K.; Adhikari, B.R.; Stamatopoulos, C.A.; Zhan, Y.; Wu, S.; Dong, Z.; Di, B. Comparison of Different Machine Learning Methods for Debris Flow Susceptibility Mapping: A Case Study in the Sichuan Province, China. *Remote Sens*. 2020, 12, 295. <https://doi.org/10.3390/rs12020295>
47. Wang, R.; Gu, J. Impact of LUCC on Vegetation Carbon Storage in Wuhu during 2000-2009. *Environmental Science and Management*, 2012, 37(6), 153-157.
48. Wang, R. Y.; Lin, P. A.; Chu, J. Y.; Tao, Y. H.; Ling, H. C. A decision support system for Taiwan's forest resource management using Remote Sensing Big Data. *Enterprise Information Systems*, 2021, 1-22. <https://doi.org/10.1080/17517575.2021.1883123>
49. Wang, Z. *Spatial and Temporal Dynamics of Forest Carbon Storage and Influencing Factors Based on CASA Model in Hangzhou*. Zhejiang Agriculture and Forestry University, 2021, <https://doi.org/10.27756/d.cnki.gzjlx.2021.000252>.

50. Wang, L.; Zhu, R.; Yin, Z.; Chen, Z.; Fang, C.; Lu, R.; Zhou, J.; Feng, Y. Impacts of Land-Use Change on the Spatio-Temporal Patterns of Terrestrial Ecosystem Carbon Storage in the Gansu Province, Northwest China. *Remote Sens.* 2022, 14, 3164. <https://doi.org/10.3390/rs14133164>
51. Wu, B. L.; Sun, H.; Shi, J. N.; Zhang, Y. T.; Shi, L. J. Dynamic change and prediction of vegetation cover in Shenzhen, China from 2000 to 2018. *Chinese Journal of Applied Ecology*, 2020. 31(11), 3777-3785. <https://doi.org/10.13287/j.1001-9332.202011.012>.
52. Xu, J.; Chen, D.; Li, W. L.; Wei, W. Study of vegetation net primary productivity in Gannan based on light use efficiency model. *Pratacultural Science*, 2019, 36(10), 2455-2465. <https://doi.org/10.11829/j.issn.1001-0629.2018-0018>
53. Yang, H.; Wu, B.; Zhang, J.; Lin, D.; Chang, S. Research progress on carbon sequestration function and carbon storage of forest ecosystem. *Journal of Beijing Normal University (Natural Science Edition)*, 2005, 02, 172-177. <https://doi.org/10.3321/j.issn:0476-0301.2005.02.018>
54. Yang Y. H.; Shi, Y.; Sun, W. J.; Chang, J. F.; Zhu, J. X.; Chen, L. Y.; Wang, X.; Guo, Y. P.; Zhang, H.T.; Yu, L. F.; Zhao, S. Q.; Xu, K.; Zhu, J. L.; Shen, H. H.; Wang, Y. Y.; Peng, Y. F.; Zhao, X.; Wang, X. P.; Hu, H. F.; Chen, S. P.; Huang, M; Wen, X. F.; Wang, S. P.; Zhu, B; Niu, S. L.; Tang, Z. Y.; Liu, L. L.; Fang J.Y., Terrestrial carbon sinks in China and around the world and their contribution to carbon neutrality. *Science China: Life Science*, 2022, 65, 861-895. <https://doi.org/10.1007/s11427-021-2045-5>.
55. Yu, G.; Hao, T.; Zhu, J. Discussion on action strategies of China's carbon peak and carbon neutrality. *Bulletin of Chinese Academy of Sciences*, 2022, 37(4), 423-434. <https://doi.org/10.16418/j.issn.1000-3045.20220121001>
56. Yu, Y.; Wang, X. G., Estimation of urban green space carbon sink for ecosystem service function. *Xi'an Univ. of Arch. & Tech. (Natural Science Edition)*, 2021, 01, 95-102. <https://doi.org/10.15986/j.1006-7930.2021.01.013>.
57. Zhang, J.B.; Zhou, S.W. Interpretation on carbon neutrality system. *Huadian Technology*, 2021, 43(06),1-10. <https://doi.org/10.3969/j.issn.1674-1951.2021.06.001>
58. Zhang, M.; Yuan, N.; Lin, H.; Liu, Y.; Zhang, H. Quantitative estimation of the factors impacting spatiotemporal variation in NPP in the Dongting Lake wetlands using Landsat time series data for the last two decades. *Ecological Indicators*, 2022, 135, 108544. <https://doi.org/10.1016/j.ecolind.2022.108544>
59. Zhang, F.; Tian, X.; Zhang, H.; Jiang, M. Estimation of Aboveground Carbon Density of Forests Using Deep Learning and Multisource Remote Sensing. *Remote Sens.* 2022, 14, 3022. <https://doi.org/10.3390/rs14133022>
60. Zhao, R.; Du, Q. Study on the Landcover Changes Based on GIS and RS Technologies: A Case Study of the Sanjiangyuan National Nature Reserve in the Hinterland Tibet Plateau, China. *Journal of Geoscience and Environment Protection*, 2022, 10, 140-150. <https://doi.org/10.4236/gep.2022.101010>.
61. Zhou, J.; Hu, Y.; Zhou, Y.; Yu, L. A design of carbon-sink model of urban landscape vegetation driven by remote sensing. *Acta Ecologica Sinica*, 2010, 30(20), 5653-5655.

62. Zhou, Z.; Ding, Y.; Liu, S.; Wang, Y.; Fu, Q.; Shi, H. Estimating the Applicability of NDVI and SIF to Gross Primary Productivity and Grain-Yield Monitoring in China. *Remote Sens.* 2022, 14, 3237. <https://doi.org/10.3390/rs14133237>
63. Zhu, W.Q.; Pan, Y.Z.; Long, Z.H.; Chen, Y.H.; Li, J.; Hu, H.B. Estimating Net Primary Productivity of Terrestrial Vegetation Based on GIS and RS : A Case Study in Inner Mongolia, China. *Journal of Remote Sensing*, 2005, 03, 300-307.
64. Zhu, W.Q.; Pan, Y.Z.; He, H.; Yu, D.Y.; Hu, H.B. Simulation of maximum light use efficiency of typical vegetation in China. *Scientific Bulletin*, 2006, 51(06), 700-706.

